Published in final edited form as:

J Immunol. 2015 November 15; 195(10): 4760–4770. doi:10.4049/jimmunol.1500979.

UNC-45A Is a Nonmuscle Myosin IIA Chaperone Required for NK Cell Cytotoxicity via Control of Lytic Granule Secretion

Yoshie Iizuka[*], **Frank Cichocki**[†], **Andrew Sieben**[*], **Fabio Sforza**[‡], **Razaul Karim**[§], **Kathleen Coughlin**[*], **Rachel Isaksson Vogel**[*], **Riccardo Gavioli**[‡], **Valarie McCullar**[†], **Todd Lenvik**[†], **Michael Lee**[§], **Jeffrey Miller**[†], and **Martina Bazzaro**[*]

[*]Department of Obstetrics, Gynecology and Women's Heath, University of Minnesota Twin Cities, Minneapolis, MN 55455

[†]Hematology, Oncology and Transplantation, University of Minnesota, Minneapolis, MN 55455

[‡]Department of Life Sciences and Biotechnology, University of Ferrara, 44121 Ferrara, Italy

[§]Department of Neuroscience, University of Minnesota, Minneapolis, MN 55455

Abstract

NK cell's killing is a tightly regulated process under the control of specific cytoskeletal proteins. This includes Wiskott-Aldrich-Syndrome protein, Wiskott-Aldrich-Syndrome protein-interacting protein, cofilin, Munc13-4, and nonmuscle myosin IIA (NMIIA). These proteins play a key role in controlling NK-mediated cytotoxicity either via regulating the attachment of lytic granules to the actin-based cytoskeleton or via promoting the cytoskeletal reorganization that is requisite for lytic granule release. UNC-45A is a highly conserved member of the UNC-45/CRO1/She4p family of proteins that act as chaperones for both conventional and nonconventional myosin. Although we and others have shown that in lower organisms and in mammalian cells NMIIA-associated functions, such as cytokinesis, cell motility, and organelle trafficking, are dependent upon the presence of UNC-45A, its role in NK-mediated functions is largely unknown. In this article, we describe UNC-45A as a key regulator of NK-mediated cell toxicity. Specifically we show that, in human NK cells, UNC-45A localize at the NK cell immunological synapse of activated NK cells and is part of the multiprotein complex formed during NK cell activation. Furthermore, we show that UNC-45A is disposable for NK cell immunological synapse formation and lytic granules reorientation but crucial for lytic granule exocytosis. Lastly, loss of UNC-45A leads to reduced NMIIA binding to actin, suggesting that UNC-45A is a crucial component in regulating human NK cell cytoskeletal dynamics via promoting the formation of actomyosin complexes.

Natural killer cells are critical for immune responses against viral infections and cancer (1). NK cell-mediated cytotoxicity begins with the formation of an active NK cell immunological synapse (NKIS) between the effector and the target cell and culminates with

Address correspondence and reprint requests to Dr. Martina Bazzaro, Department of Obstetric, Gynecology and Women's Health, Room 490, 420 Delaware Street S.E., Minneapolis, MN 55455. mbazzaro@umn.edu.

The online version of this article contains supplemental material.

Disclosures

The authors have no financial conflicts of interest.

the release of lytic granule content for target cell killing (2–4). Unlike CTLs, which are present in small precursor frequencies and must undergo differentiation and expansion before target cell killing, NK cells are ready-to-kill cells armed with a constitutive pool of lytic granules. Thus, NK cell killing is a tightly regulated process that is particularly sensitive to cytoskeletal dynamics (4–8). A number of cytoskeletal-associated proteins including Wiskott-Aldrich-Syndrome protein (WASp), WASp-interacting protein, cofilin, Munc13-4, and nonmuscle myosin IIA (NMIIA) are involved in the stepwise cytoskeletal reorganization that is requisite for lytic granule release (3, 6, 9, 10). Mutations in the genes coding for these proteins severely compromise NK cell-mediated cytotoxicity and result in severe immunodeficiency (11, 12).

In lower organisms and in mammalian cells, NMIIA-assisted functions including cytokinesis, cell motility, and organelle trafficking are dependent upon the presence of its cochaperone UNC-45A (13–17). UNC-45A is a highly conserved member of the UCS (UNC-45/Cro1/She4p) protein family, which plays a crucial role in chaperone motor protein assembly (18, 19). Our group and others have recently shown that UNC-45A interacts with and affects the folding and stability of myosins including NMIIA via direct binding with myosin heads (19). This allows for its efficient binding to actin. Although high UNC-45A RNA expression levels have been reported in NK cells (20), the cellular localization and functional relevance of UNC-45 protein in NK cells has yet to be described. Given the functional dependency of NK cells on cytoskeletal dynamics in general and for NMIIA function in particular, we sought to investigate the role of the NMIIA cochaperone UNC-45A during NK cell–mediated cytotoxicity.

In this study, we show that UNC-45A protein is abundantly expressed in human NK cells, where it interacts with lytic granules and binds to NMIIA. Furthermore, we show that small hairpin RNA (shRNA)-mediated silencing of UNC-45A severely affects NK cell cytotoxicity. Lastly, our results show that impairment of NK cell cytotoxicity in UNC-45A knockdown cells is not due to an inability of these cells to form active immunological synapses, but to a deficiency in lytic granule secretion via a mechanism involving alteration of actomyosin contractility.

Materials and Methods

Isolation of cells from peripheral blood

Human subjects were used as per the Institutional Review Board approval and with their consent. Adult peripheral blood was obtained from healthy donors. PBMCs were isolated by centrifugation using a Ficoll–Paque Premium. NK cells were negatively selected from PBMCs using Clini MACS CD3 Reagent (273-01, Miltenyi Biotec), and cultured at 37°C with 5% CO_2 in a 3.5:1 (v:v) mix of DMEM (11995; Life Technologies) and F-12 (11765; Life Technologies) containing 10% human heat-inactive serum (HP1022; Valley Biomedical), 25 μM 2-ME (21985-023; Invitrogen), 50 μM ethanolamine (E0135; Sigma), 1.7 μg/l sodium selenite (214485; Sigma), 20 mg/l ascorbic acid, and 1000 U/ml human IL-2 (200-02; Peprotech). Monocytes were isolated by positive magnetic selection using CD14 microbeads (Miltenyi Biotech) according to the manufacturer’s instructions. B, T, and NK

cells were all isolated by negative magnetic bead selection according to the manufacturer's instructions.

Modulation of UNC-45A expression levels in human NK cells

For UNC-45A silencing in YT, NKL, and peripheral blood NK (p-NK) cells, scramble and UNC-45A shRNAs (5′-CTGGAAGATTACGACAAAGCA-3′ #1 and 5′-CCACCTCAAGCTGGAAGATTA-3′ #2) were inserted into the GFP-containing lentiviral YT cells or GFP-containing lenti-pEF empty vector (NKL and p-NK cells). Plasmids were cotransfected with the VSVG envelope, and the delta-8.9 and infection were performed as we previously described (21). Forty-eight hours postinfection, GFP^+ $CD3^-CD56^+$ p-NK cells were sorted and collected using a FACSAria II (BD Biosciences). For UNC-45A silencing in NK-92 cells, scramble and UNC-45A shRNA lentiviral particles were purchased from Santa Cruz (sc-90291) and used according to the manufacturer's instructions. For UNC-45A overexpression in NK cells, lenti-pEF-GFP-SIN and lenti-pEF-UNC-45GFP were cotransfected with the VSVG envelope, and the delta-8.9 plasmids and infection were performed as we previously described (21).

Quantitative RT-PCR

Total RNA was purified using the Qiagen RNeasy Mini kit (Qiagen). cDNA was generated by SuperScript III Transcriptase (Invitrogen) and used as template for quantitative real-time PCR using SYBR Green Master Mix (Roche) and the Applied Biosystems 7300 Real-Time PCR System. The primers used for quantitative real-time PCR were 5′-TCCGAGGCAAAGAAGGTGCCATC-3′ and 5′-ACCGCTTTAATCAGGAGGGTCAGGG-3′ for *UNC-45A* and 5′-TGCACCACCAACTGCTTAGC-3′ and 5′-GGCATGGACTGTGGTCATGAG-3′ for GAPDH.

NK cell lines

YT, NKL, 721.221, and K562 cells were cultured at 37°C with 5% CO_2 in RPMI 1640 with 10% FBS. A total of 100 U/ml human IL-2 was added for NKL cells. NK-92 cells (American Type Culture Collection) were cultured in Alpha MEM with 12.5% horse serum, 12.5% FBS, 0.1 mM 2-ME, and 500 U/ml human IL-2.

Chemicals, Abs, and plasmids

Chemicals, reagents and plasmids were obtained from the following: Ficoll–Paque Premium (GE Healthcare), Clini-MACS CD3 reagents and CD14 microbeads (Miltenyi Biotech), Blebbistatin, ionomycin, apyrase and PMA (Sigma-Aldrich), brefeldin and monesin (Pharmingen), nonmuscle actin and ATP (Cytoskeleton), CellTracker Orange (Life Technologies), anti–UNC-45A (Enzo Life Sciences), anti-perforin, anti–CD3-PerCP, anti–CD56-allophycocyanin and anti–CD107a-PE (BD Biosciences), anti-NMIIA (Covance), anti–p-NMIIA H chain (Ser1943) (Cell Signaling), anti-NMIIA L chain (Ser20) (Abcam), anti-lysosomal associated membrane protein 1 (LAMP-1), anti-actin (Sigma), PE-conjugated anti-perforin (BD Pharmingen), mouse monoclonal anti-β actin for immunofluorescence (IF) (Sigma), Alexa Fluor 647–conjugated donkey anti-mouse IgG,

Texas red goat anti-mouse IgG, Texas red-goat anti-rabbit IgG, FITC-donkey, and anti-mouse IgG (Jackson Immunoresearch Laboratories).

[^{51}Cr]-release assay

NK cell cytotoxic activity was tested in standard 5-h [^{51} Cr]-release assays as previously described (2). In brief, 721.221 and K562 target cells were labeled with 0.1 μCi/10^6 cells of $Na_2{}^{51}CrO_4$ for 90 min at 37°C and incubated with effector cells at the indicated ratio. Per each condition, the percentage specific lysis was calculated as follows: (exp. cpm – spontaneously released cpm)/(total cpm – spontaneously released cpm). Total cpm were assessed by complete lysis of target cells by using 1% Triton X-100.

Western blotting and coimmunoprecipitation—For Western blot analysis, cell lysates (10–20 μg) and lysosomal fractions (50 μl) from each sample were separated by SDS-PAGE, transferred to polyvinylidene difluoride membranes, and subjected to Western blot analysis using the indicated Abs according to the manufacturer's recommendations. For coimmunoprecipitation experiments, human NK cells were lysed into lysis buffer (50 mM Tris, pH 7.4, 150 mM NaCl, 1% Nonidet P-40, 1X protease inhibitor mixture, 1X phosphatase inhibitor mixture). The lysates were precleared and precipitated with primary Ab and protein A/G beads. Pellets were washed three times with ice-cold lysis buffer and analyzed by SDS-PAGE.

Immunofluorescence microscopy—For analysis of UNC-45A subcellular localization, YT NK cells overexpressing UNC-45A-GFP fusion protein or primary NK cells were incubated with 721.221 or K562 target cells, respectively, at a 2:1 ratio in suspension for 30 min and adhered to poly-L-lysine–coated glass slides (Polyprep; Sigma-Aldrich) for 15 min. After fixation and permeabilization, cells were stained with the anti-myosin IIA and anti-UNC-45A (primary cells only) Abs, followed by FITC-conjugated donkey anti-mouse IgG or by Texas red–conjugated goat anti-rabbit IgG for UNC-45A and NMIIA, respectively, and analyzed via fluorescence microscopy. For measurement of lytic granules polarization, scramble and UNC-45A knockdown YT cells (GFP^+) were incubated with or without 721.221 target cells at a 2:1 ratio. Cells were adhered to poly-L-lysine-coated cover glasses for 15 min, followed by fixation with 0.4% paraformaldehyde, staining with mouse anti-perforin Ab, and followed by Texas red–conjugated anti-mouse IgG Ab and analyzed via fluorescence microscopy. The percentage of cells with polarized lytic granules was determined by number of perforin polarized NK cells out of total number of NK target conjugates. Images were taken with a Nikon Eclipse T200 fluorescent microscope using a plan Apo VC 60X/1.4 ∞ 10.7 WD 0.13 oil lens (Nikon) and acquired using a NIS-Element F 3.3 camera and software. Alternatively, images were taken with an Olympus BX2 upright microscope equipped with a Fluoview 1000 confocal scan head. A UPlanApo N 60X/1.42 NA objective and a pixel size of 0.118 μm was used. Enhanced GFP (EGFP) was excited with a 488-nm laser and emission collected between 505 and 525 nm. For Texas red, a 543-nm laser was used for excitation and emission collected between 560 and 660 nm. Alexa Fluor 647 was excited with a 635-nm laser and emission collected between 655 and 755 nm. Images were taken with sequential excitation.

Isolation of lytic granules from NK cells—Postnuclear lysate (PNL) and crude lysosomal fraction (CLF) were obtained by centrifugation at 1000 × *g* of homogenized lysates (from 1×10^8 YT cells) and pelleting of lytic granules in PNL at 18,000 × *g* as previously described (22). Lysosomal fractions (*a–f*) were obtained by Optiprep density gradient centrifugation using the Lysosomal Isolation Kit (Sigma-Aldrich) according to the manufacturer's instructions. Fraction of 0.2 ml was harvested for subsequent analysis.

Formation and measurement of effector-target conjugates—Scramble and UNC-45A knockdown YT cells (GFP^+) were mixed with an equal volume of CellTracker Orange–loaded 721.221 target cells in a 5-ml polystyrene round-bottom tube at a 2:1 ratio. Cells were centrifuged at 20 × *g* for 1 min, incubated in 5% CO2 at 37°C for 15 min without agitation. At the end of incubation time, the cells were vortexed for 3 s at maximum vortex speed and immediately fixed with ice-cold 2% paraformaldehyde/PBS. Flow cytometry (BD FACSCalibur) was used to measure conjugate frequency as previously described (23).

Evaluation of NK cell morphology after UNC-45A knockdown—For analysis of NK cell morphology in UNC-45A knockdown cells, stable YT cells expressing either scramble or UNC-45A knockdown (KD#1 and KD#2) were adhered to poly-L-lysine-coated glass slides for 15 min. After fixation and permeabilization, cells were stained with DAPI and analyzed via phase-contrast and fluorescence microscopy.

Measurement of cell viability in UNC-45A knockdowns NK cells

For measurement of NK cell viability after UNC-45A knockdown, stable YT cells expressing either scramble or UNC-45A knockdown (KD#1 and KD#2) were seeded at a density of 5000 cells/well (12-well plate) and counted at the indicated time points in a hemocytometer in the presence of trypan blue to exclude dead cells.

CD 107a surface expression analysis

Scramble and UNC-45A knockdown YT cells were either mock-treated (DMSO) or treated with 10–25 ng/ml PMA and 0.5 μg/ml ionomycin for 5 h in the presence of the PE-conjugated anti-CD107a Ab and the protein transport inhibitors monensin and brefeldin as previously described (2). At the end of the incubation period, cells were washed, fixed, and analyzed using a FACSCalibur.

Granzyme A release assay

Granzyme A has an esterase activity, which can be measured using the substrate BLT ester as previously described (24). Specifically, scramble and UNC-45A knockdown NKL cells were either mock-treated (DMSO) or treated with 25 ng/ml PMA and 0.5 μg/ml ionomycin for 5 h at 37°C. Cell-free supernatant and total cell lysate obtained by repeated freeze-thaw were assayed for esterase (granzyme A) activity using BLT as a substrate. The specific release of serine esterase was measured by incubation of 45 μl cell-free supernatant with 180 μl 0.2 M Tris-HCl, pH 8.1 containing 0.2 mM BLT and 0.22 mM dithio-bis-nitrobenzoic acid. The percentage of specific enzymatic release was calculated on the basis of the total enzymatic content (total lysate). Absorbance was read using a spectrophotometer at 405/690 nm (ELISA reader 190; Molecular Devices).

IFN-γ secretion assay

Scramble and UNC-45A knockdown NK-92 cells were rested in IL-2–free medium for 16 h after stimulation with (or without) 10 ng/ml IL-12 and 100 ng/ml IL-18 for 4, 7, and 16 h. The supernatant was collected and IFN-γ secretion was measured using a commercial ELISA kit (DY285; R&D Systems).

Measurement of intracellular perforin by FACS analysis

For intracellular measurement of perforin expression levels, YT NK cells transduced with either shRNA-scramble or shRNA targeting two different UNC-45A regions (1 and 2), original YT cells, or isotype-treated (anti-mouse IgG) YT cells were fixed, permeabilized, and stained with PE-conjugated anti-perforin Ab (556434; BD Pharmingen). At the end of the incubation period, cells were washed and analyzed using a BD LSR II flow cytometer.

Myosin II-actin functional assay

ATP-dependent myosin II–actin filament interaction was measured by adapting a recently described method for quantification of myosin II–actin binding (15). Specifically, UNC-45A knockdown (KD#1 and KD#2) or UNC-45A–GPF–expressing YT cells were lysed in buffer containing 20 mM Tris, pH 7.0, 0.5% Triton, 25 mM KCl, 5 mM MgCl2, 0.5 mM EGTA, 1 mM PMSF, and 1X proteinase inhibitor mixture. After elimination of unbroken cells and debris (100,000 × *g* for 30 min at 4°C), supernatants were further spun at 100,000 × *g* for 30 min at 4°C using a TL100 Beckman, and the supernatants supplemented with 30 μg/ml human platelet nonmuscle actin and incubated for 2 h on ice. Actin-bound myosin II was pelleted by ultracentrifugation (100,000 × *g* for 30 min at 4°C), and pellet was resuspended in high-salt buffer. After 1-h incubation on ice, actin-bound myosin was pelleted by centrifugation at 100,000 × *g* for 30 min at 4°C to release functional myosin II from the pellet. The supernatant served as input for the binding reaction. A total of 5 mM Mg-ATP and 150 μg/ml actin was added to the supernatant; then the sample was transferred to two tubes (450 μl each) and incubated for 2 h on ice. After the incubation, 10 μl apyrase (0.1 U/μl; Sigma) was added to one of the samples for ATP minus actin binding (motor domain-dependent actin binding). Ten minutes after incubation at room temperature, the samples were centrifuged at 100,000 × *g* for 30 min at 4°C. The supernatants were discarded and the pellet washed once with 100 μl lysis buffer plus 5 mM ATP either treated without or with apyrase. After centrifugation, the pellets were resuspended in 30 μl SDS-PAGE sample buffer and processed for Western blot analysis.

Cell image analysis

Images were analyzed using either ImageJ or Imaris (version 8.1.2; Bit-plane) software. For immunofluorescence analyses, thresholds were determined automatically using Costes' algorithms in the Imaris program or calculated using ImageJ. Areas analyzed were either the entirety of the NK cell, defined using phase-contrast images to determine the perimeter of the NK cell, half of the cell oriented toward the NKIS, or the polarized region of a conjugated NK cell. The polarized region was defined as a triangular area with its tips located at the edge points of the NK–target cell interface and the center of the NK cell. Granules were considered polarized if >90% of granules were localized within this area. The

mean fluorescent intensity (MFI) was defined as the quantified intensity of the fluorophores in the polarized area. To determine the amount of UNC-45A that localizes to the NKIS upon conjugation, we drew a line parallel to the cell–cell contact site through the center of the NK cell body. The ratio was defined as fluorescent intensity between the NKIS-oriented half of the cell and the entire cell body. Perforin localization was quantified by segregating the NK cell into four quadrants. Quadrants were defined by placing the intersection of perpendicular lines at the center of the NK cell, with the lines parallel to the sides of the field of vision. The upper left quadrant was labeled Q1, the upper right Q2, the bottom left Q3, and the bottom right Q4. Perforin puncta were then counted for each quadrant. Arbitrary units are defined as the values generated from ImageJ analyses and are relative to each respective experiment. Perforin puncta were then counted for each quadrant. Cell morphology was analyzed as cell area and circularity using ImageJ software, with the cell perimeter defined using the ImageJ drawing tool. Cell circularity was defined as the ratio between the area of the cell and its perimeter ($4\pi \times \text{area/perimeter}^2$). The ratio ranges from 0 to 1, with 1 indicating a perfect circle and values progressing toward 0 representing an increasingly elongated shape. For all of the quantifications, between 10 and 30 cells/condition were analyzed. Experiments were repeated a minimum of three times.

Statistical analysis

Results are reported as mean ± SD of three or more independent experiments. Unless otherwise indicated, statistical significance was assessed by two-tailed Student *t* test using Prism (V.4 GraphPad, San Diego, CA) and Excel. The level of significance was set at $p < 0.05$.

Results

UNC-45A binds to and colocalizes with NMIIA in NK cells

Microarray analysis indicates a pattern of high UNC-45A RNA expression in human blood cells and in NK cells in particular (20). Thus, we first investigated whether UNC-45A is expressed at protein levels in human lymphocytes. To this end, lysates from $CD14^+$ monocytes, $CD19^+$ B cells, $CD4^+$ T cells, $CD8^+$ T cells, $CD3^-CD56^+$ NK (p-NK) cells, and three NK cell lines YT, NKL, and NK-92 were subjected to Western blot analysis using an mAb against UNC-45A. As shown in Fig. 1 A, we found that UNC-45A is expressed at protein levels in all the cell subsets analyzed, confirming the presence of UNC-45A protein in human lymphocytes.

Next, we tested the hypothesis that UNC-45A is a binding partner of NMIIA in the NK cell context. To this end, lysates from NK cell lines and primary p-NK cells were immunoprecipitated with an anti-UNC-45A mAb, and binding to NMIIA was evaluated by Western blot. As shown in Fig. 1B, UNC-45A coimmunoprecipitates with NMIIA in both human YT and NKL NK cell lines and primary p-NK cells. To test whether UNC-45A has a potential role in controlling NK-mediated functions, we investigated UNC-45A subcellular localization in activated human NK cells. To this end, human YT NK cells expressing UNC-45A-GFP fusion protein and primary NK cells were incubated with 721.221 or K562 target cells, respectively, and the effector–target conjugates were stained with Abs against

UNC-45A and/or NMIIA. Immunofluorescence microscopy revealed that UNC-45A and NMIIA colocalize at the effector–target cell interface of activated YT and p-NK cells (Fig. 1C, *left* and *right panels*, respectively). Specifically, image quantification analyses revealed that ~60% of the total UNC-45A present in the YT cells localizes at the NKIS and >70% of the total UNC-45A present in p-NK cells localizes at the NKIS (Fig. 1D, *top panel*). Furthermore, image quantification analyses revealed that in both YT and p-NK cells, >70% of the total UNC-45A colocalizes with NMIIA in NK cells (Fig. 1D, *bottom panel*). Taken together, this suggests that UNC-45A is a likely candidate for mediating NMIIA-associated functions in NK cells.

UNC-45A colocalizes with perforin in activated NK cells and associates with lytic granules

Given that UNC-45A colocalizes with and binds to NMIIA in NK cells (Fig. 1), we next wanted to evaluate whether UNC-45A associates with perforin-containing lytic granules in NK cells. To test this, YT NK cells were transduced with UNC-45A–GFP fusion protein and incubated with 721.221 target cells and conjugates stained with a mAb against perforin to allow for visualization. UNC-45A shows a ubiquitous subcellular localization and a partial overlap with perforin granules in unengaged NK cells (Supplemental Fig. 1). In activated NK cells, however, UNC-45A is polarized at the effector–target cell interface, where it colocalizes with perforin (Fig. 2A, *left panels*). Specifically, image quantification analyses revealed that ~70% of the total cellular UNC-45A colocalizes with perforin at the effector-target cell interface (Fig. 2A, *right panel*).

Next, we biochemically tested whether UNC-45A interacts with lytic granules. Cell lysates from YT NK cells were separated by density gradient fractionation (22) and the derived fractions, along with PNL and CLFs, were analyzed by Western blot using Abs against UNC-45A, NMIIA, and LAMP-1. UNC-45A was found specifically in the lytic granule preparation containing NMIIA and LAMP-1 (Fig. 2B). Quantification of the relative abundance of UNC-45A, NMIIA, and LAMP-1 in NK cell-derived lysosomal fractions is shown in Fig. 2C. Taken together, these results suggest that UNC-45A is a component of a multiprotein complex formed during NK cell activation and may play a role during NKIS formation and/or lytic granule exocytosis.

UNC-45A knockdown impairs the cytotoxic activity of human NK cells

Next, we wanted to test whether the presence of the NMIIA cochaperone UNC-45A is required for NK cell–mediated cytotoxicity. To this end, UNC-45A was knocked down via lentiviral-mediated delivery of shRNAs targeting multiple UNC-45A regions in NK cell lines and p-NK cells. Efficiency of UNC-45A knockdown was evaluated by Western blot and RT-PCR analysis showing a reduction in UNC-45A expression of ~90% in YT cells (Fig. 3A) and ~75% in p-NK cells (Fig. 3B). Next, we evaluated the effect of UNC-45A knockdown on the capability of NK cell lines and p-NK cells to kill target cells. YT cells infected with lentiviral particles carrying either shRNA scramble or shRNAs directed against two different UNC-45A sequences (1 and 2) were incubated with 721.221 target cells and residual specific lysis evaluated by [^{51}Cr]-release assays. UNC-45A knockdown resulted in a dramatic reduction in NK cell cytotoxicity relative to the scramble controls (Fig. 3C, *left panel*). A similar reduction in target cell lysis was observed with specific pharmacological

inhibition of NMIIA using blebbistatin (Fig. 3C, *middle panel*). Quantification of the reduction in YT NK cell-mediated lysis as a result of UNC-45A knockdown is shown in Fig. 3C (*right panel*). Next, we tested whether a similar effect could be observed upon UNC-45A knockdown in primary NK cells. Primary $CD3^{-}CD56^{+}$ NK cells isolated from healthy donors were infected with lentivirus harboring scramble or UNC-45A shRNA, sorted, and incubated with K562 target cells. UNC-45A knockdown resulted in significant impairment of cytotoxic capabilities in primary NK cells in [^{51}Cr]-release assays (Fig. 3D, *left* and *middle panels*). Quantification of the reduction in primary NK cell lysis resulting from UNC-45A knockdown is shown in Fig. 3D (*right panel*). To exclude the possibility that the reduction in the cytotoxic capability of UNC-45A knockdown NK cells was due to impairment of cell viability, we evaluated both cell morphology and proliferative activity in scramble and UNC-45A knockdown YT cells. Our results show that UNC-45A knockdown did not affect NK cell morphology as evaluated by determination of cells' area and circularity or proliferation rate (Supplemental Figs. 2, 3, respectively). Together, these data suggest that UNC-45A plays a critical role in regulating NK-mediated cytotoxicity without interfering with cell viability.

UNC-45A knockdown does not prevent formation of effector-target conjugates

Reduction in cytotoxic capabilities in NK cell lines and primary NK cells after UNC-45A knockdown (Fig. 3), along with its colocalization with NMIIA at the NKIS (Figs. 1, 2), suggests that the loss of UNC-45A might hinder cell killing by perturbing the formation of effector-target conjugates. To test this hypothesis, we transduced YT NK cells with lenti-pEF-shRNAmir targeting scramble sequences or two different UNC-45A regions, incubated with CellTracker Orange–loaded 721.221 target cells and the number of effector–target conjugates in control and UNC-45A knockdowns evaluated using two different approaches. In the first approach, the number of green:red (YT NK721.221) conjugates was manually counted under the microscope and reported as the number of conjugates per field. We did not observe a significant difference in terms of ability to form conjugates in control versus UNC-45A knockdown NK cells (Fig. 4A). To confirm this result, the effect of UNC-45A silencing on conjugate formation was measured by FACS analysis. YT NK cells were transduced with scramble shRNAmir or UNC-45A shRNAmir were incubated with CellTracker Orange–loaded 721.221 target cells. After fixation, FACS analysis was performed to determine the number of conjugates, defined as the green-red double-positive population. We did not observe a difference in terms of the ability of NK cells to form conjugates after UNC-45A knockdown (Fig. 4B). Specifically, quantification of the percentage of effector-target conjugates at $t = 0$ and at $t = 10$ min revealed the absence of a statistically significant difference in UNC-45A knockdown cells versus control (Fig. 4C). Thus, the role of UNC-45A in NK cell cytotoxicity is independent of NKIS formation.

UNC-45A knockdown does not prevent lytic granule polarization and does not alter perforin levels

After NKIS formation, polarization of the lytic granules at the cell–cell contact site is a required event for NK cell–mediated cytotoxicity. Because UNC-45A knockdown did not hinder NKIS formation (Fig. 4), we next evaluated whether the reduced lytic capacity of NK cells after UNC-45A knockdown is due to inefficient lytic granule polarization. To test this

hypothesis, we incubated YT NK cells transduced with scramble or UNC-45A shRNAmir with 721.221 target cells and visualized recruitment of perforin to the NKIS via fluorescence microscopy. In unengaged NK cells, perforin was localized throughout the cytoplasm (Supplemental Fig. 4), whereas in engaged NK cells, perforin-containing lytic granules were found to localize at the IS in both scramble and UNC-45A knockdown cells (Fig. 5A). Quantification of the percentage of cells with polarized lytic granules in scramble versus UNC-45A knockdown (#1, #2) is shown in Fig. 5B. Next, we addressed the question whether UNC-45A knockdown would alter intracellular levels of perforin in NK cells. To this end, we first quantified the MFI in the perforin-polarized regions in scramble versus UNC-45A knockdown YT cells. As shown in Fig. 5C, we did not observe any statistically significant difference in terms of MFI in scramble versus UNC-45A knockdown cells. To confirm this result, we next measured the intracellular levels of perforin in scramble versus UNC-45A knockdown YT cells via FACS analysis. As shown in Fig. 5D, the intracellular amount of perforin in UNC-45A knockdown cells did not differ from the one in scramble or isotype-treated controls. Taken together, this suggests that UNC-45A is not required for polarization of perforin-containing lytic granules to the NKIS nor does it alter intracellular levels of perforin in NK cells.

UNC-45A is obligate for NK cell degranulation and IFN-γ secretion

NK cell–mediated cytotoxicity occurs when, after polarization at the NKIS contact site, lytic granules are secreted into the space between NK cell and target. The lack of an observable effect on NKIS formation (Fig. 4) and lytic granule polarization (Fig. 5) in NK cells after UNC-45A knockdown suggested that the loss of UNC-45A might reduce NK cell–mediated cytotoxicity by preventing lytic granule secretion at the NKIS site. To test this hypothesis, we transduced NKL and NK-92 cells with either scramble shRNA or shRNAs targeting UNC-45A. The efficiency of UNC-45A knockdown in NKL and NK-92 cells was evaluated by Western blot analysis showing a reduction in UNC-45A expression of ~60% in NKL cells (Fig. 6A, *left panel*) and ~90% in NK-92 cells (Fig. 6A, *right panel*). Cells were then either mock-treated (DMSO) or treated with 50 ng/ml PMA and 0.5 μg/ml ionomycin. The effect of PMA/ionomycin stimulation on NK cell degranulation was evaluated by measuring the increase in surface expression of the lysosome marker CD107a. Our results show that UNC-45A knockdown is associated with reduced expression of CD107a on the surface of NKL (Fig. 6B, *left panel*) and NK-92 (Fig. 6C, *left panel*) cells relative to scramble controls. Quantification of CD107a surface expression (% of control) for YT and NK-92 is shown in Fig. 6B and 6C (*right panels*), respectively.

To directly determine the impact of UNC-45A on secretion of lytic granule content, we measured the effect of UNC-45A knockdown on granzyme release in NK cells in response to PMA/ionomycin stimulation. UNC-45A knockdown resulted in a dramatic reduction in granzyme A secretion in both NKL and NK-92 NK cells (Fig. 6D, *left* and *right panels*, respectively). Next, we evaluated the impact of modulating the UNC-45A expression levels in NK cells on IFN-γ secretion. To this end, NK-92 cells transduced with either shRNA-scramble or shRNA consisting of a pool (shRNA-UNC-45A pool) of three UNC-45A–specific shRNAs were either mock-treated or treated with 10 ng/ml IL-12 and 100 ng/ml IL-18 over a period of 4, 7, or 16 h. At the end of each incubation time, residual IFN-γ was

measured by ELISA assay. As shown in Fig. 6E, UNC-45A knockdown resulted with statistically significant reduction in IFN-γ by NK cells starting as early as 4 h from treatment and observable for up to 16 h.

Taken together, these show that UNC-45A knockdown causes impaired NK-mediated cytotoxicity by preventing lytic granules exocytosis and prevents IFN-γ secretion.

UNC-45A is required for ATP-dependent NMIIA interaction with actin

An intact actin–myosin network is crucial during NK cell–mediated cytotoxicity and allows for efficient delivery and fusion of secretory granules to the cell membrane. Previous studies have shown that the selective NMIIA inhibitor blebbistatin severely abrogates NK cell cytotoxicity via reducing the affinity of NMIIA heads for myosin (25, 26). Thus, we tested whether the lack of NK cell degranulation in the absence of UNC-45A occurs through unfolding and/or destabilization of NMIIA. To address this hypothesis, we measured the levels of NMIIA and its phosphorylated forms after UNC-45A knockdown in NK cells. YT NK cells transduced with either shRNA-scr amble or shRNA targeting UNC-45A were similar with respect to total NMIIA expression levels, pNMIIA H chain levels, and pNMIIA L chain levels (Fig. 7A). Thus, it appears that, at least in the NK cell context, UNC-45A does not play a role in NMIIA stabilization or folding. Recent reports using breast cancer cell lines suggest that UNC-45A plays a role in modulating NMIIA–actin functional interactions by controlling the ATP-sensitive interaction of NMIIA with actin filaments (15). Thus, we tested whether the absence of UNC-45A in NK cells is associated with a reduction in NMIIA–actin binding capacity. As shown in Fig. 7B (*left panel*), UNC-45A knockdown did not affect the total expression levels of NMIIA within NK cells. However, when lysates from either scramble of UNC-45A knockdown YT NK cells were exposed to exogenous actin in presence (+) of the ATP diphosphohydrolase apyrase, this resulted with a dramatic decrease in the NMIIA-actin interactions as compared with controls (Fig. 7B, *middle* and *right panels*). Furthermore, when we performed the complementary experiments by over-expressing GFP-tagged UNC-45A in the same cells, we observed the opposite effect: a significant in NMII-actin binding over controls (Fig. 7C). Quantification of actin–NMIIA binding for the earlier described experiments is given in Fig. 7D. To further confirm the requirement of UNC-45A for NMIIA and actin interaction, we visualized UNC-45A, NMIIA, and actin in UNC-45A–GFP–expressing YT NK cells conjugated with 721.221 cells. As shown in Fig. 7E, UNC-45A, NMIIA, and actin all appear to localize at the interface between effector and target cell. Taken together, our data suggest that reduced lytic granule exocytosis in NK cells lacking UNC-45A may be caused by impairments in cellular cytoskeletal dynamics.

Discussion

Perturbing of the actin-based microfilaments within NK cells has dramatic consequences on their activities including cytotoxicity. Thus, understanding of mechanisms regulating the cytoskeletal dynamic within NK cell is fundamental for the understanding of NK cell's functions in both the physiological and the pathological context.

Exposure of NK cells to the NMIIA inhibitor blebbistatin, for instance, causes a block of the myosin heads in a state of low affinity for actin resulting with impaired NK-mediated cytotoxicity (2, 22, 27–29). Mutations in *WAS* (encoding WASp) on the other side are associated with reduced perforin granule polarization at the NKIS due to inefficient F-actin branching (5, 30–33). Furthermore, loss of WASp-interacting protein functions causes defects in NK cell–mediated killing via increased proteasome-mediated WASp degradation and its mislocalization (32, 34–37). Lastly, inefficient tethering of lytic granules to the plasma membrane in NK cells carrying mutations in the *UNC13D* gene is associated with a complete loss of NK cell–mediated cytotoxicity (11, 38–41).

Functional assembly of the evolutionally conserved NMIIA requires both a heat shock protein and a highly conserved member of the UCS protein family to act together to chaperone motor assembly (13, 17, 19, 42, 43). The UCS proteins are a family of cochaperone molecules that interact with the well-established chaperone molecule heat shock protein 90 and with both conventional and nonconventional myosin heads to ensure their proper activity during cytokinesis, cell motility, cell contraction, as well as organelle trafficking within the cellular compartment.

In mammalian cells, NMIIA plays a crucial role in both cytokinesis and cell migration, and we and others have recently shown that UNC-45A is required for the sustaining of high proliferation rate and invasive properties of ovarian and breast cancer cells (15, 44).

One of the first events after NK cell activation is rearrangement of the actin cytoskeleton and translocation of NMIIA to NKIS where it associates with perforin-containing lytic granules promoting the release of their content (4). In this article, we demonstrate that UNC-45A is expressed in human NK cells where it colocalizes and interacts with NMIIA. Furthermore, UNC-45A and NMIIA colocalization are maintained in activated NK cells where both proteins are found at the NKIS. In NK cells, the formation of an active IS followed by the polarization of lytic granules to the target interface in an NMIIA-independent fashion (4). In this study, we found that UNC-45A colocalizes with lytic granules in both resting and activated NK cells, polarizes along with perforin to the NKIS upon target engagement, and is abundantly represented in the same fractions as both NMIIA and the lysosomal luminal protein LAMP-1 (45). We also found that loss of UNC-45A results in a severe impairment of NK cell cytotoxic functions, which was not associated with a decreased frequency of effector–target cell conjugates or inefficient polarization of lytic granules containing perforin to the NKIS. Rather, UNC-45A knockdown negatively impacted the ability of NK cells to secrete lytic granules in response to target cell recognition. Mechanistically, modulation of the UNC-45A expression levels in human NK cells corresponded with a dramatic reduction in ATP-dependent interaction with NMIIA.

Together our data demonstrate that UNC-45A is a component of the NK cell cytoskeleton and plays a key role during NK cell–mediated cytotoxicity in a step between approach of the lytic granules to the NKIS and their release at the effector–target cell interspace. Although the nature of this step is yet to be identified, we propose that the effect of UNC-45A in controlling lytic granule exocytosis could be either dependent or independent from its effect on regulating NMIIA activity, and that these two scenarios are not mutually exclusive. One

possibility is that UNC-45A plays a role in assisting NMIIA in transporting the lytic granules through F-actin at the IS to facilitate their fusion to the cell membrane. In a separate scenario, UNC-45A acts independent of NMIIA and is part of the multisubunit complex that regulates the events of priming, docking, and fusion of lytic granules to the cell membrane leading up to target cell killing.

Supplementary Material

Refer to Web version on PubMed Central for supplementary material.

Acknowledgments

We are grateful to Dr. Henry F. Epstein, who prematurely died, for friendship and support. We thank Drs. Ritz and Reynolds (Dana-Farber Cancer Institute) and Dr. Strominger (Harvard University) for the gift of the NKL cell line. We thank Dr. Koho Iizuka (University of Minnesota) for the gift of the lenti-pEF-GFP-SIN. We thank Dr. Guillermo Marques (University of Minnesota Imaging Center) for assistance with image analysis and quantification.

This work was supported by the Department of Defense Ovarian Cancer Research Program OC093424 and by the Randy Shaver Cancer Research and Community Fund (to M.B.).

Abbreviations used in this article

CLF	crude lysosomal fraction
EGFP	enhanced GFP
IF	immunofluorescence
LAMP-1	anti-lysosomal associated membrane protein 1
MFI	mean fluorescent intensity
NKIS	NK cell immunological synapse
NMIIA	nonmuscle myosin IIA
p-NK	peripheral blood NK
PNL	postnuclear lysate
shRNA	small hairpin RNA
shRNAmir	microRNA-adapted shRNA
UCS	UNC-45/CRO1/She4p
WASp	Wiskott-Aldrich-Syndrome protein

References

1. Reyburn H, Mandelboim O, Valés-Goméz M, Sheu EG, Pazmany L, Davis DM, Strominger JL. Human NK cells: their ligands, receptors and functions. Immunol. Rev. 1997; 155:119–125. [PubMed: 9059887]
2. Andzelm MM, Chen X, Krzewski K, Orange JS, Strominger JL. Myosin IIA is required for cytolytic granule exocytosis in human NK cells. J. Exp. Med. 2007; 204:2285–2291. [PubMed: 17875677]

3. Krzewski K, Chen X, Orange JS, Strominger JL. Formation of a WIP-, WASp-, actin-, and myosin IIA-containing multiprotein complex in activated NK cells and its alteration by KIR inhibitory signaling. J. Cell Biol. 2006; 173:121–132. [PubMed: 16606694]
4. Orange JS, Harris KE, Andzelm MM, Valter MM, Geha RS, Strominger JL. The mature activating natural killer cell immunologic synapse is formed in distinct stages. Proc. Natl. Acad. Sci. USA. 2003; 100:14151–14156. [PubMed: 14612578]
5. Wulfing C, Purtic B, Klem J, Schatzle JD. Stepwise cytoskeletal polarization as a series of checkpoints in innate but not adaptive cytolytic killing. Proc. Natl. Acad. Sci. USA. 2003; 100:7767–7772. [PubMed: 12802007]
6. Mace EM, Orange JS. Lytic immune synapse function requires filamentous actin deconstruction by Coronin 1A. Proc. Natl. Acad. Sci. USA. 2014; 111:6708–6713. [PubMed: 24760828]
7. Na BR, Kim HR, Piragyte I, Oh HM, Kwon MS, Akber U, Lee HS, Park DS, Song WK, Park ZY, et al. TAGLN2 regulates T cell activation by stabilizing the actin cytoskeleton at the immunological synapse. J. Cell Biol. 2015; 209:143–162. [PubMed: 25869671]
8. Anton IM, Jones GE, Wandosell F, Geha R, Ramesh N. WASP-interacting protein (WIP): working in polymerisation and much more. Trends Cell Biol. 2007; 17:555–562. [PubMed: 17949983]
9. Elstak ED, Neeft M, Nehme NT, Voortman J, Cheung M, Goodarzifard M, Gerritsen HC, van Bergen En Henegouwen PM, Callebaut I, Basile Gde Saint, Sluijs Pvan der. The muncl3-4-rab27 complex is specifically required for tethering secretory lysosomes at the plasma membrane. Blood. 2011; 118:1570–1578. [PubMed: 21693760]
10. Antón IM, de la Fuente MA, Sims TN, Freeman S, Ramesh N, Hartwig JH, Dustin ML, Geha RS. WIP deficiency reveals a differential role for WIP and the actin cytoskeleton in T and B cell activation. Immunity. 2002; 16:193–204. [PubMed: 11869681]
11. Cichocki F, Schlums H, Li H, Stache V, Holmes T, Lenvik TR, Chiang SC, Miller JS, Meeths M, Anderson SK, Bryceson YT. Transcriptional regulation of Muncl3-4 expression in cytotoxic lymphocytes is disrupted by an intronic mutation associated with a primary immunodeficiency. J. Exp. Med. 2014; 211:1079–1091. [PubMed: 24842371]
12. Meeths M, Chiang SC, Wood SM, Entesarian M, Schlums H, Bang B, Nordenskjöld E, Björklund C, Jakovljevic G, Jazbec J, et al. Familial hemophagocytic lymphohistiocytosis type 3 (FHL3) caused by deep intronic mutation and inversion in UNC13D. Blood. 2011; 118:5783–5793. [PubMed: 21931115]
13. Ni W, Hutagalung AH, Li S, Epstein HF. The myosin-binding UCS domain but not the Hsp90-binding TPR domain of the UNC-45 chaperone is essential for function in *Caenorhabditis elegans* . J. Cell Sci. 2011; 124:3164–3173. [PubMed: 21914819]
14. Price MG, Landsverk ML, Barral JM, Epstein HF. Two mammalian UNC-45 isoforms are related to distinct cytoskeletal and muscle-specific functions. J. Cell Sci. 2002; 115:4013–4023. [PubMed: 12356907]
15. Guo W, Chen D, Fan Z, Epstein HF. Differential turnover of myosin chaperone UNC-45A isoforms increases in metastatic human breast cancer. J. Mol. Biol. 2011; 412:365–378. [PubMed: 21802425]
16. Hoppe T, Cassata G, Barral JM, Springer W, Hutagalung AH, Epstein HF, Baumeister R. Regulation of the myosin-directed chaperone UNC-45 by a novel E3/E4-multiubiquitylation complex in C. elegans. Cell. 2004; 118:337–349. [PubMed: 15294159]
17. Barral JM, Bauer CC, Ortiz I, Epstein HF. Unc-45 mutations in *Caenorhabditis elegans* implicate a CRO1/She4p–like domain in myosin assembly. J. Cell Biol. 1998; 143:1215–1225. [PubMed: 9832550]
18. Lee CF, Melkani GC, Bernstein SI. The UNC-45 myosin chaperone: from worms to flies to vertebrates. Int. Rev. Cell Mol. Biol. 2014; 313:103–144. [PubMed: 25376491]
19. Shi H, Blobel G. UNC-45/CRO1/She4p (UCS) protein forms elongated dimer and joins two myosin heads near their actin binding region. Proc. Natl. Acad. Sci. USA. 2010; 107:21382–21387. [PubMed: 21115842]
20. Su AI, Wiltshire T, Batalov S, Lapp H, Ching KA, Block D, Zhang J, Soden R, Hayakawa M, Kreiman G, et al. A gene atlas of the mouse and human protein-encoding transcriptomes. Proc. Natl. Acad. Sci. USA. 2004; 101:6062–6067. [PubMed: 15075390]

21. Iizuka YM, Somia NV, Iizuka K. Identification of NK cell receptor ligands using a signaling reporter system. Methods Mol. Biol. 2010; 612:285–297. [PubMed: 20033648]
22. Sanborn KB, Rak GD, Maru SY, Demers K, Difeo A, Martignetti JA, Betts MR, Favier R, Banerjee PP, Orange JS. Myosin IIA associates with NK cell lytic granules to enable their interaction with F-actin and function at the immunological synapse. J. Immunol. 2009; 182:6969–6984. [PubMed: 19454694]
23. Kanwar N, Wilkins JA. IQGAP1 involvement in MTOC and granule polarization in NK-cell cytotoxicity. Eur. J. Immunol. 2011; 41:2763–2773. [PubMed: 21681737]
24. Galandrini R, Micucci F, Tassi I, Cifone MG, Cinque B, Piccoli M, Frati L, Santoni A. Arf6: a new player in FcgammaRIIIA lymphocyte-mediated cytotoxicity. Blood. 2005; 106:577–583. [PubMed: 15817676]
25. Kovács M, Tóth J, Hetényi C, Málnási-Csizmadia A, Sellers JR. Mechanism of blebbistatin inhibition of myosin II. J. Biol. Chem. 2004; 279:35557–35563. [PubMed: 15205456]
26. Allingham JS, Smith R, Rayment I. The structural basis of blebbistatin inhibition and specificity for myosin II. Nat. Struct. Mol. Biol. 2005; 12:378–379. [PubMed: 15750603]
27. Sanborn KB, Mace EM, Rak GD, Difeo A, Martignetti JA, Pecci A, Bussel JB, Favier R, Orange JS. Phosphorylation of the myosin IIA tailpiece regulates single myosin IIA molecule association with lytic granules to promote NK-cell cytotoxicity. Blood. 2011; 118:5862–5871. [PubMed: 22123909]
28. Sanborn KB, Rak GD, Mentlik AN, Banerjee PP, Orange JS. Analysis of the NK cell immunological synapse. Methods Mol. Biol. 2010; 612:127–148. [PubMed: 20033638]
29. Ramamurthy B, Yengo CM, Straight AF, Mitchison TJ, Sweeney HL. Kinetic mechanism of blebbistatin inhibition of nonmuscle myosin lib. Biochemistry. 2004; 43:14832–14839. [PubMed: 15544354]
30. Helgeson LA, Prendergast JG, Wagner AR, Rodnick-Smith M, Nolen BJ. Interactions with actin monomers, actin filaments, and Arp2/3 complex define the roles of WASP family proteins and cortactin in coordinately regulating branched actin networks. J. Biol. Chem. 2014; 289:28856–28869. [PubMed: 25160634]
31. Sadhukhan S, Sarkar K, Taylor M, Candotti F, Vyas YM. Nuclear role of WASp in gene transcription is uncoupled from its ARP2/3-dependent cytoplasmic role in actin polymerization. J. Immunol. 2014; 193:150–160. [PubMed: 24872192]
32. Ramesh N, Massaad MJ, Kumar L, Koduru S, Sasahara Y, Anton I, Bhasin M, Libermann T, Geha R. Binding of the WASP/N-WASP-interacting protein WIP to actin regulates focal adhesion assembly and adhesion. Mol. Cell. Biol. 2014; 34:2600–2610. [PubMed: 24797074]
33. Wulfing C, Davis MM. A receptor/cytoskeletal movement triggered by costimulation during T cell activation. Science. 1998; 282:2266–2269. [PubMed: 9856952]
34. Martinez-Quiles N, Rohatgi R, Antón IM, Medina M, Saville SP, Miki H, Yamaguchi H, Takenawa T, Hartwig JH, Geha RS, Ramesh N. WIP regulates N-WASP-mediated actin polymerization and filopodium formation. Nat. Cell Biol. 2001; 3:484–491. [PubMed: 11331876]
35. Moreau V, Frischknecht F, Reckmann I, Vincentelli R, Rabut G, Stewart D, Way M. A complex of N-WASP and WIP integrates signalling cascades that lead to actin polymerization. Nat. Cell Biol. 2000; 2:441–448. [PubMed: 10878810]
36. Ramesh N, Anton IM, Hartwig JH, Geha RS. WIP, a protein associated with wiskott-aldrich syndrome protein, induces actin polymerization and redistribution in lymphoid cells. Proc. Natl. Acad. Sci. USA. 1997; 94:14671–14676. [PubMed: 9405671]
37. Donnelly SK, Weisswange I, Zettl M, Way M. WIP provides an essential link between Nek and N-WASP during Arp2/3-dependent actin polymerization. Curr. Biol. 2013; 23:999–1006. [PubMed: 23707428]
38. Sieni E, Cetica V, Santoro A, Beutel K, Mastrodicasa E, Meeths M, Ciambotti B, Brugnolo F, zur Stadt U, Pende D, et al. Genotype-phenotype study of familial haemophagocytic lymphohistiocytosis type 3. J. Med. Genet. 2011; 48:343–352. [PubMed: 21248318]
39. Wood SM, Meeths M, Chiang SC, Bechensteen AG, Boelens JJ, Heilmann C, Horiuchi H, Rosthøj S, Rutynowska O, Winiarski J, et al. Different NK cell-activating receptors preferentially recruit

Rab27a or Muncl3-4 to perform-containing granules for cytotoxicity. Blood. 2009; 114:4117–4127. [PubMed: 19704116]

40. Côte M, Ménager MM, Burgess A, Mahlaoui N, Picard C, Schaffner C, Al-Manjomi F, Al-Harbi M, Alangari A, Deist FLe, et al. Muncl8-2 deficiency causes familial hemophagocytic lymphohistiocytosis type 5 and impairs cytotoxic granule exocytosis in patient NK cells. J. Clin. Invest. 2009; 119:3765–3773. [PubMed: 19884660]
41. Elstak ED, Loo Mte, Tesselaar K, van Kerkhof P, Loeffen J, Grivas D, Hennekam E, Boelens JJ, Hoogerbrugge PM, van der Sluijs P, et al. A novel Dutch mutation in UNC13D reveals an essential role of the C2B domain in muncl3-4 function. Pediatr. Blood Cancer. 2012; 58:598–605. [PubMed: 21755595]
42. Barral JM, Hutagalung AH, Brinker A, Hartl FU, Epstein HF. Role of the myosin assembly protein UNC-45 as a molecular chaperone for myosin. Science. 2002; 295:669–671. [PubMed: 11809970]
43. Wesche S, Arnold M, Jansen RP. The UCS domain protein She4p binds to myosin motor domains and is essential for class I and class V myosin function. Curr. Biol. 2003; 13:715–724. [PubMed: 12725728]
44. Bazzaro M, Santillan A, Lin Z, Tang T, Lee MK, Bristow RE, Shih IeM, Roden RB. Myosin II co-chaperone general cell UNC-45 over-expression is associated with ovarian cancer, rapid proliferation, and motility. Am. J. Pathol. 2007; 171:1640–1649. [PubMed: 17872978]
45. Cohnen A, Chiang SC, Stojanovic A, Schmidt H, Claus M, Saftig P, Janßen O, Cerwenka A, Bryceson YT, Watzl C. Surface CD107a/LAMP-1 protects natural killer cells from degranulation-associated damage. Blood. 2013; 122:1411–1418. [PubMed: 23847195]

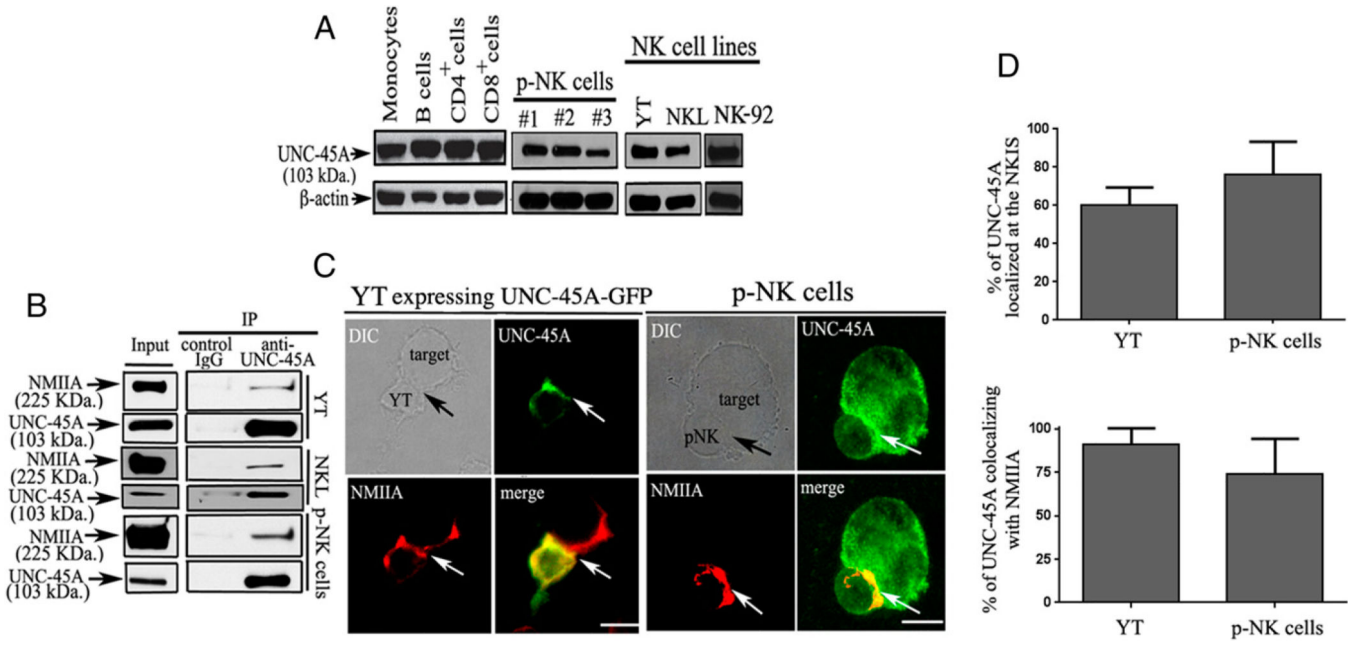

FIGURE 1.

UNC-45A expression and localization in NK cells. (**A**) Western blot analysis of UNC-45A in lysates from primary monocytes, $CD19^+$ B cells, $CD4^+$ T cells, $CD8^+$ T cells, and $CD3C^-D56^+$ NK cells from the peripheral blood and the YT, NKL, and NK-92 NK cell lines. β-Actin was used as loading control. The blots presented are representative of three independent experiments with three different blood donors. (**B**) UNC-45A immunoprecipitated from lysates of YT and NKL NK cell lines or primary p-NK cells with an anti-UNC-45A mAb. Coimmunoprecipitated NMIIA was detected by Western blot analysis using an anti-NMIIA polyclonal Ab. Immunoprecipitation with nonspecific IgG was performed as a control. (**C**, *left panels*) YT NK cells overexpressing a UNC-45A–GFP fusion protein were incubated with 721.221 target cells. After fixation, cells were stained with an anti-NMIIA polyclonal Ab and Texas red goat anti-rabbit IgG and analyzed by fluorescence microscopy. (*Right panels*) p-NK cells incubated with K562 target cells. After fixation, cell conjugates were stained with anti–UNC-45A and anti-NMIIA Abs followed by FITC-conjugated donkey anti-mouse IgG or by Texas red-conjugated goat anti-rabbit IgG for UNC-45A and NMIIA, respectively, and analyzed by fluorescence microscopy. Arrows indicate NKISs. Scale bars, 5 μm. (**D**, *top panel*) Quantification of the percentage of UNC-45A localized at the NKIS out of the total present in the cells for YT and p-NK. (*Bottom panel*) Quantification of the percentage of UNC-45A colocalizing with NMIIA out of the total present in the cells for YT and p-NK.

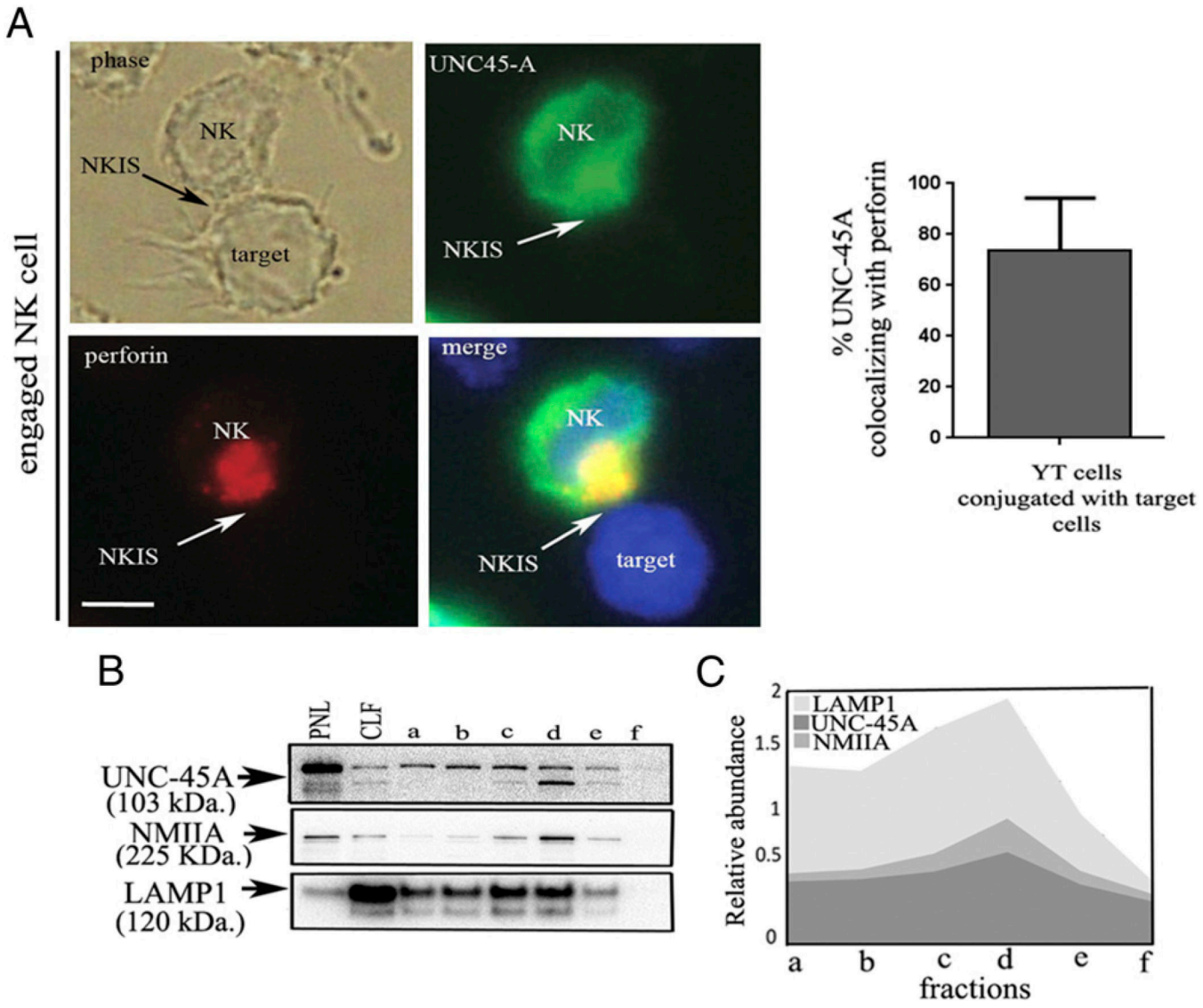

FIGURE 2.

UNC-45A colocalizes with perforin and interacts with lytic granules in engaged NK cells. (**A**, *left panels*) YT NK cells expressing a GFP–UNC-45A fusion protein were incubated in presence of 721.221 target cells for 30 min. After fixation and permeabilization, unengaged (*left*) or engaged (*right*) NK cells were stained with anti-perforin Ab and Texas red-conjugated anti-mouse IgG and analyzed by phase-contrast and fluorescence microscopy. Arrows indicate NKISs. Scale bars, 5 μM. (*Right panel*) Quantification of the percentage of UNC-45A colocalizing with perforin out of the total present in YT cells. (**B**) Fractions from density gradient separation of lytic granules in YT NK cells from least dense (*lane a*) to most dense (*lane f*), PNL, and CLF were used for Western blot analysis with Abs against UNC-45A, NMIIA, and LAMP-1. (**C**) Quantification of relative abundance of UNC-45A, NMIIA, and LAMP-1 in NK cell-derived lysosomal fractions.

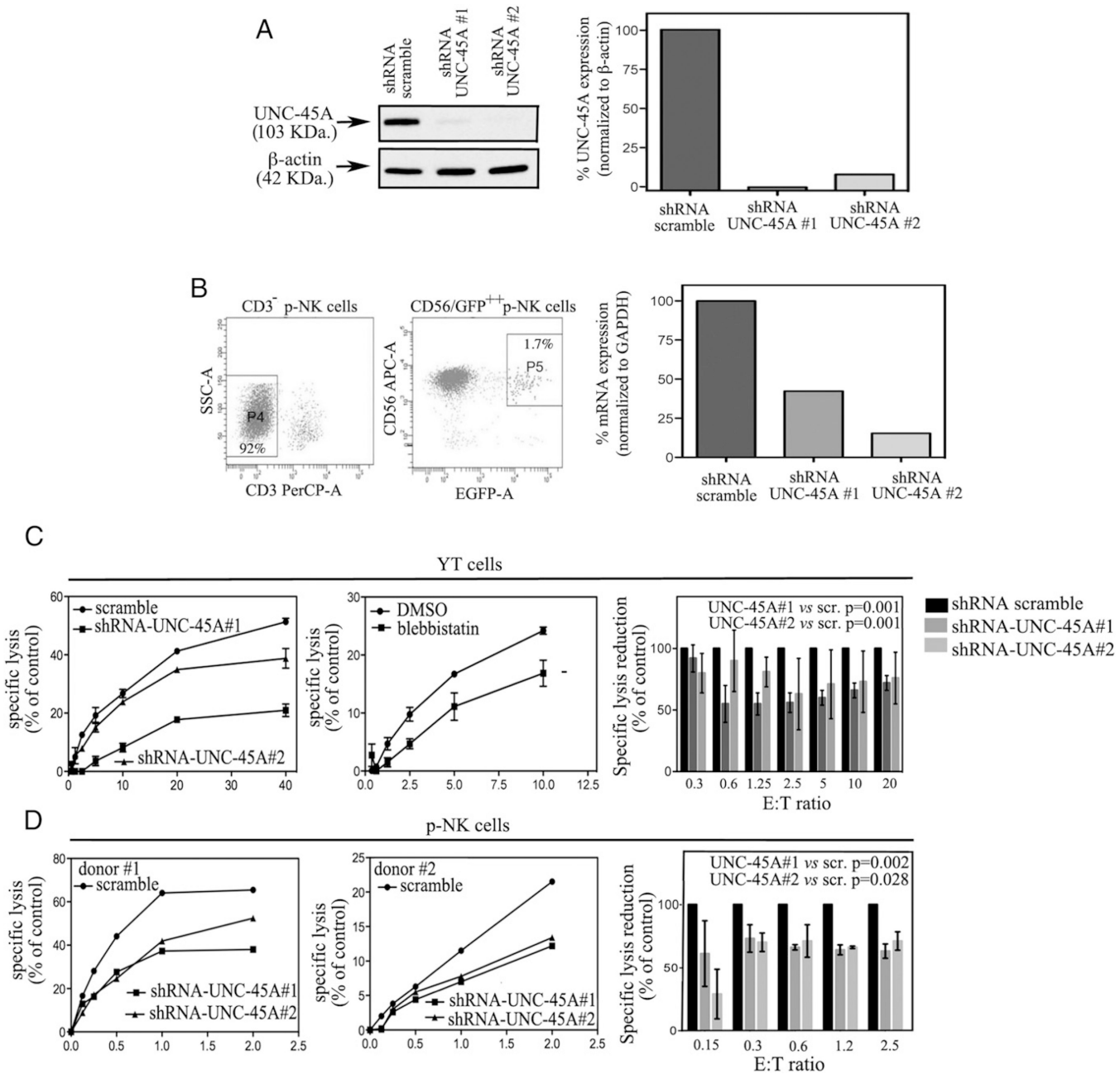

FIGURE 3.

UNC-45A knockdown hinders NK cell–mediated cytotoxicity. (**A**, *left panel*) Western blot analysis of UNC-45A expression in YT cells transduced with either shRNA-scramble or shRNA targeting two different UNC-45A regions (1 and 2). β-Actin was used as a loading control. (*Right panel*) Quantification of the percentage of UNC-45A expression normalized to β-actin. (**B**, *left panels*) UNC-45A knockdown in primary $CD3^-$ lymphocytes (P4) virally infected with lenti-pEF-UNC45-shRNAmir (1 and 2). Forty-eight hours postinfection, GFP^+ $CD3^-CD56^+$ cells were sorted (P5) for quantification of UNC-45A levels. (*Right panel*) Efficiency of UNC-45A knockdown in primary NK cells measured by quantitative RT-PCR. The mRNA values reported are relative to the control gene (GAPDH) and normalized to

control-treated cells. (**C**, *left panel*) Residual specific lysis in YT cells infected with lentiviral particles carrying either shRNA scramble or shRNAs directed against two different UNC-45A sequences (1 and 2) incubated with 721.221 target cells at the indicated ratios. A representative experiment is shown. (*Middle panel*) Residual specific lysis in YT cells either mock- (DMSO) or blebbistatin (75 μM)-treated and incubated with 721.221 target cells at the indicated ratios. A representative experiment is shown. (*Right panel*) Average of five independent experiments reported as reduction in specific lysis as compared with the controls (set at 100%). (**D**, *left* and *middle panels*) Residual specific lysis in lenti-pEF-UNC45-shRNAmir (1 and 2) or scramble infected, $CD3^{-}/CD56^{+}/GFP^{+}$-sorted p-NK cells derived from healthy donors (donors 1 and 2) incubated with K562 target cells at the indicated ratios. (*Right panel*) Average of three independent experiments reported as reduction compared with controls (set at 100%). For all experiments (conducted in triplicates), specific lysis was assessed by [^{51}CR]-release assay. Statistical significance was set at $p = 0.05$.

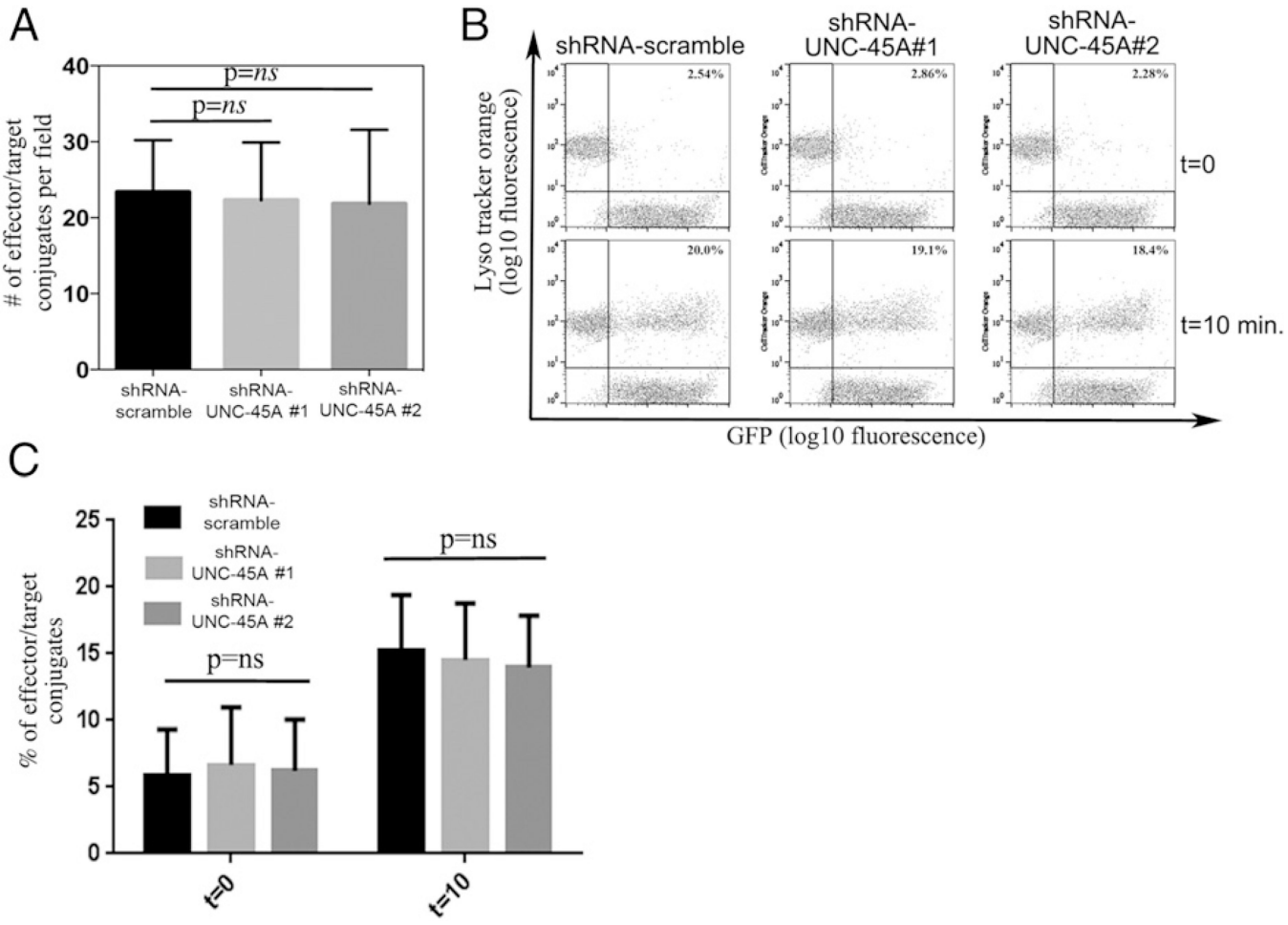

FIGURE 4.

UNC-45A knockdown does not prevent effector-target conjugate formation. (**A**) YT NK cells transduced with lenti-pEF-UNC45-shRNAmir targeting either scramble or two different UNC-45A (1 and 2) regions were incubated with CellTracker Orange-loaded 721.221 target cells. The number of conjugates (effector green/target red) per condition were counted under fluorescence microscopy and reported as the number of conjugates per field. The average of three independent experiments is shown. (**B**) YT NK cells transduced with lenti-pEF-UNC45-shRNAmir targeting either scramble of two different UNC-45A (1 and 2) regions were incubated with CellTracker Orange–loaded 721.221 target cells. Samples were either immediately fixed (t_0) or fixed after 10 min of incubation (t_{10}). The number of conjugates was quantified by FACS analysis. The average of three independent experiments is shown. (**C**) Quantification of percentage of effector-target conjugates in shRNA scramble or shRNA UNC-45A (1 and 2) at $t = 0$ and $t = 10$ min.

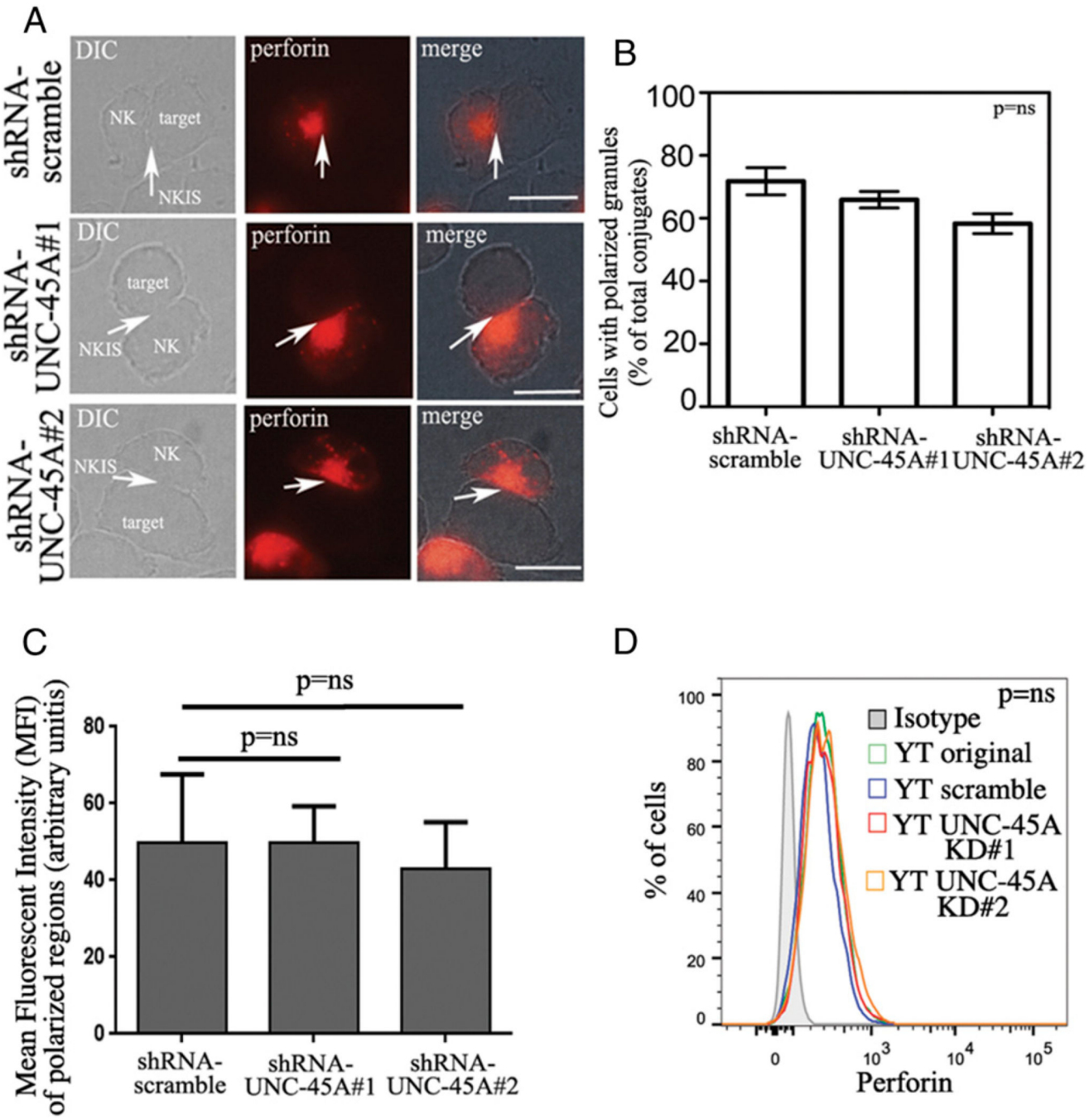

FIGURE 5.

UNC-45A knockdown does not interfere with lytic granules polarization or with perforin expression levels. (**A**) YT NK cells transduced with either shRNA-scramble or shRNA targeting two different UNC-45A regions (1 and 2) were incubated with 721.221 target cells. After fixation, cells were stained with an anti-perforin mAb followed by Texas red goat anti-mouse IgG and analyzed by fluorescence microscopy. A representative experiment is shown. Arrows indicate NKISs. Scale bars, 5 μm. (**B**) Quantification of polarized granules per condition reported as the percentage of cells with polarized lytic granules out of the total

number of conjugates. The averages of three independent experiments are shown. (**C**) Quantification of MFI in polarized regions in YT cell transduced with either scramble or shRNAs targeting UNC-45A regions (1 and 2). (**D**) Intracellular staining of perforin in YT cell transduced with either scramble of shRNAs targeting UNC-45A regions (1 and 2) or original, or treated with anti-mouse IgG as iso-type control and analyzed by FACS using a PE-conjugated anti-perforin Ab.

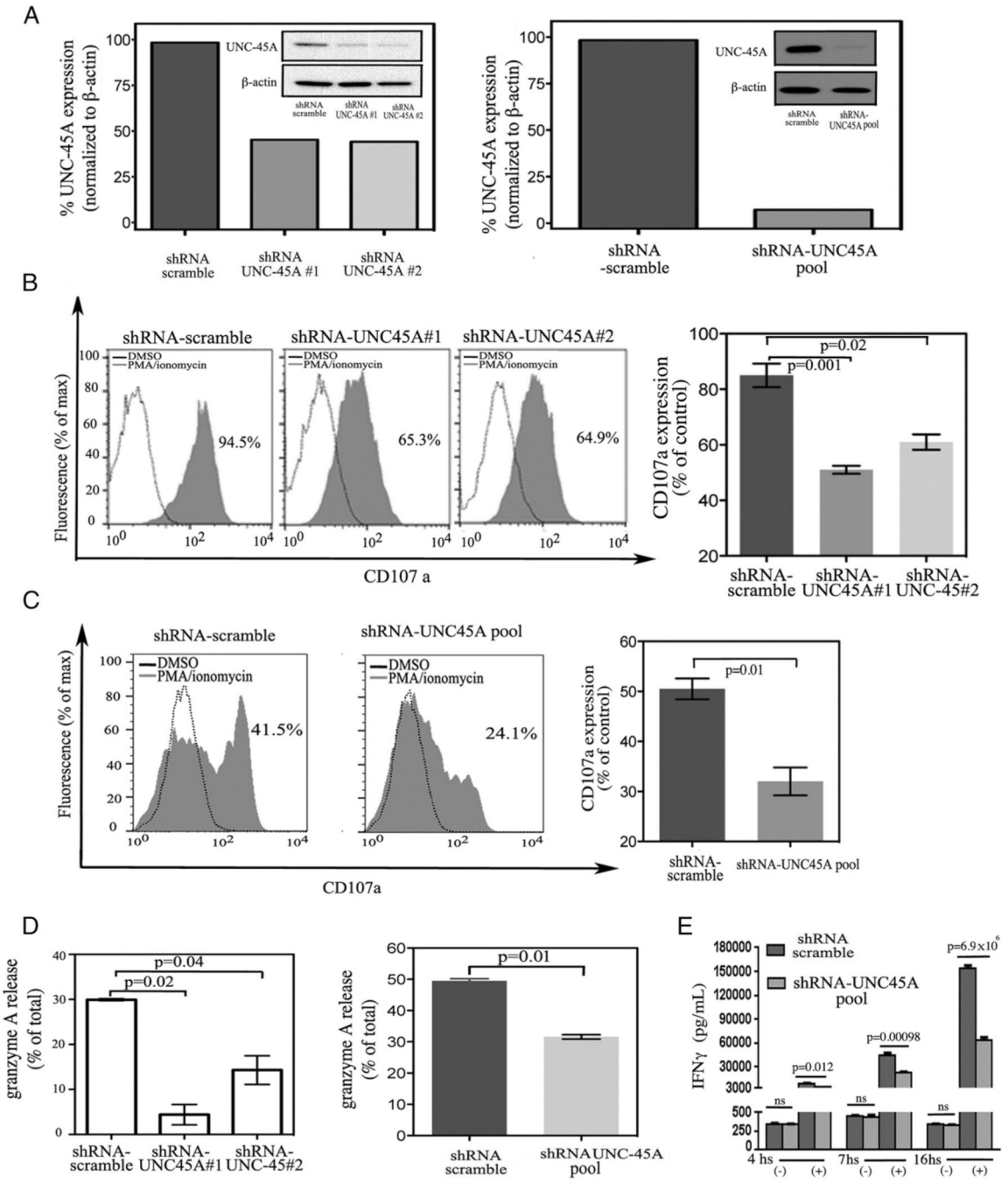

FIGURE 6.

UNC-45A knockdown prevents lytic granule secretion and IFN-γ release in NK cells. (**A**) UNC-45A protein expression levels in lysates of NKL (*left panel*) and NK-92 (*right panel*) cells upon transduction with either shRNA-scramble or shRNA targeting two different UNC-45A regions (1 and 2) and in NK-92 NK cells after transduction with shRNA scramble or shRNA consisting of a pool (shRNA-UNC-45A pool) of three 19- to 25-nt UNC-45A–specific shRNAs. β-Actin was used as a loading control. (**B**) NKL cells transduced with either shRNA-scramble or shRNA targeting two different UNC-45A regions (1 and 2) and

either mock-treated (DMSO) or treated in presence of 25 ng/ml PMA and 0.5 μg/ml ionomycin. Surface CD107a expression was analyzed by FACS. A representative experiment is shown. (*Right panel*) Quantification of CD107a expression averaged from three independent experiments. (**C**, *left panels*) NK-92 cells transduced with either shRNA-scramble or shRNA consisting of a pool (shRNA-UNC-45A pool) of three 19- to 25-nt UNC-45A–specific shRNAs either mock-treated (DMSO) or treated in the presence of 50 ng/ml PMA and 0.5 μg/ml ionomycin. The effect of PMA/ionomycin stimulation on NK cells was evaluated by measuring the increase in surface expression of CD107a by FACS analysis. Representative experiment. (*Right panel*) Quantification of the CD107a expression. Average of three independent experiments. (**D***left panel*) NKL cells transduced with either shRNA-scramble or shRNA targeting two different UNC-45A regions (1 and 2) and either mock-treated (DMSO) or treated in the presence of 25 ng/ml PMA and 0.5 μg/ml ionomycin. Granzyme A release is reported as the percentage of specific release over total enzymatic content. The average of three independent experiments is shown. (*Right panel*) NK-92 cells transduced with either shRNA-scramble or shRNA consisting of a pool (shRNA-UNC-45A pool) of three 19- to 25-nt UNC-45A–specific shRNAs were either mock-treated (DMSO) or treated in the presence of 50 ng/ml PMA and 0.5 μg/ml ionomycin. Granzyme A release is reported as the percentage of specific release over total enzymatic content. The average of three independent experiments is shown. (**E**) Scramble and UNC-45A knockdown (pool) NK-92 cells mock-treated (−) or stimulated in the presence of 10 ng/ml IL-12 and 100 ng/ml IL-18 (+) over a period of 4, 7, or 16 h. Per each condition, IFN-γ secretion was measured by ELISA and expressed as IFN-γ pg/ml.

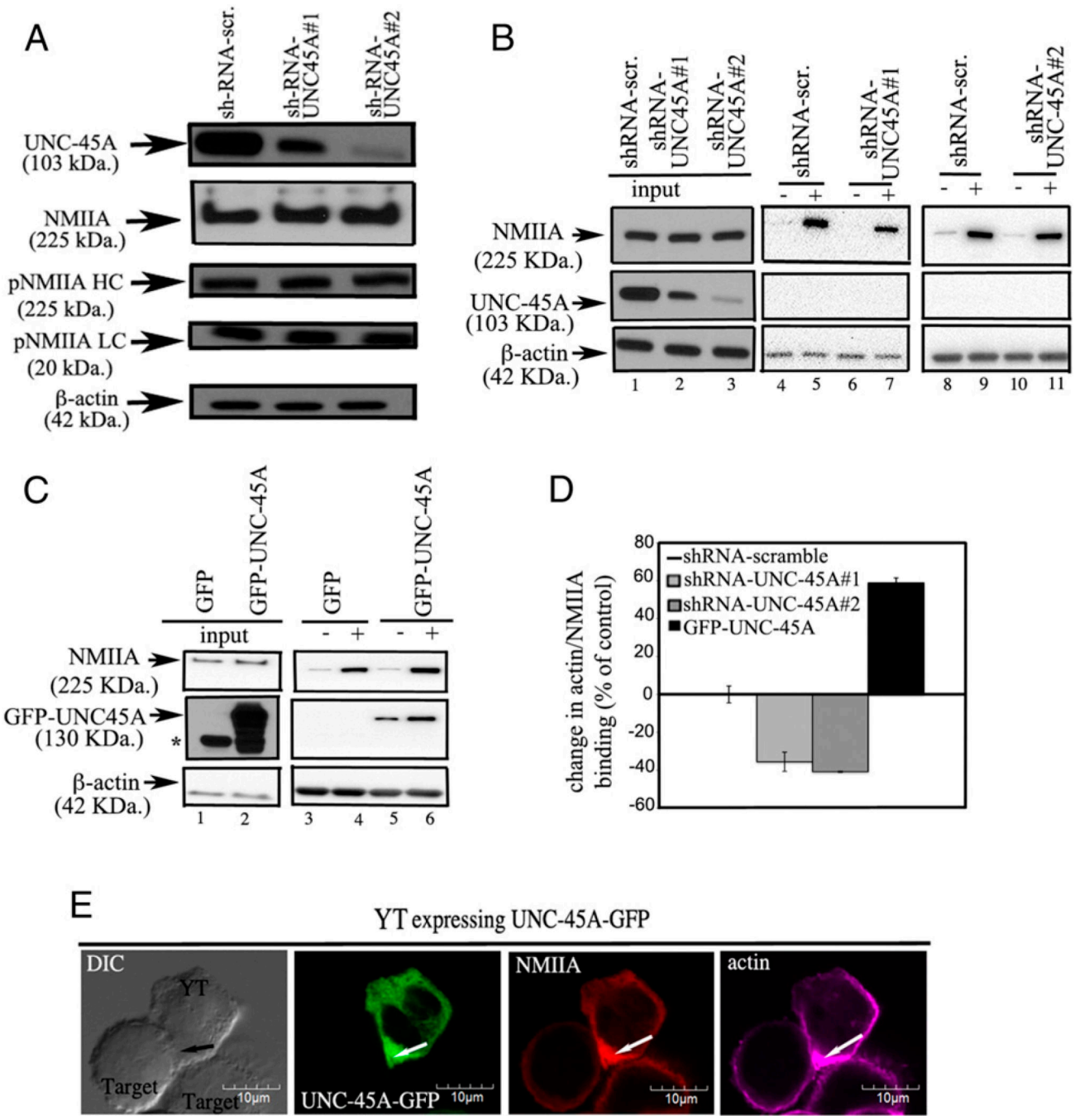

FIGURE 7.

Effect of UNC-45A knockdown on NMIIA expression levels and ATP-sensitive interactions of NMIIA with actin filaments. (**A**) Expression levels of UNC-45A, NMIIA, pNMIIA H chain (HC), and pNMIIA L chain (LC) in YT cells transduced with either shRNA-scramble or shRNA targeting two different UNC-45A regions. β-Actin was used as a loading control. (**B**) NMIIA-actin binding capability in YT cells transduced with either scramble or shRNA targeting two different UNC-45A regions in the absence (−) and presence (+) of the ATP diphosphohydrolase apyrase. (**C**) NMIIA-actin binding capability in YT cells transduced

with empty vector (lenti-pEF-GFP) or lenti-pEF-UNC-45A–GFP in the absence (−) and presence (+) of the ATP diphosphohydrolase apyrase. (**D**) Quantification of NMIIA actin-binding capability expressed as a percentage of the control (average of two independent experiments) and obtained by comparing lines 5 and 7 and 9 and 11 of (B) and lines 4 and 6 of (C). (**E**) YT NK cells expressing UNC-45A–GFP fusion protein were incubated with 721.221 target cells. After fixation, effector-target conjugates were stained with an anti-NMIIA polyclonal Ab and an anti-actin mAb followed by Texas red goat anti-rabbit IgG and Alexa Fluor 647-conjugated donkey anti-mouse IgG and analyzed by fluorescence microscopy. Arrow indicates the NKIS.